Modulation of Hexokinase Association with Mitochondria Analyzed with Quantitative Three-Dimensional Confocal Microscopy

Ronald M. Lynch, Kevin E. Fogarty, and Fredric S. Fay

Department of Physiology, University of Massachusetts Medical Center, Worcester, Massachusetts 01655

Abstract. Hexokinase isozyme I is proposed to be associated with mitochondria in vivo. Moreover, it has been suggested that this association is modulated in coordination with changes in cell metabolic state. To test these hypotheses, we analyzed the subcellular distribution of hexokinase relative to mitochondria in paraformaldehyde-fixed astrocytes using immunocytochemistry and quantitative three-dimensional confocal microscopy. Analysis of the extent of colocalization between hexokinase and mitochondria revealed that ~70% of cellular hexokinase is associated with mitochondria under basal metabolic conditions. In contrast to the immunocytochemical studies, between 15 to 40% of cellular hexokinase was found to be associated with mitochondria after fractionation of astrocyte cultures depending on the exact fractionation conditions. The discrepancy between fractionation studies and those based on imaging of distributions in fixed cells indicates the usefulness of using techniques that can evaluate the distributions of "cytosolic" enzymes in cells whose subcellular ultrastructure is not severely disrupted. To determine if hexokinase distribution is modulated in concert with changes in cell metabolism, the localization of hexokinase with mitochondria was evaluated after inhibition of glucose metabolism with 2-deoxyglucose. After incubation with 2-deoxyglucose there was an approximate 35% decrease in the amount of hexokinase associated with mitochondria. These findings support the hypothesis that hexokinase is bound to mitochondria in rat brain astrocytes in vivo, and that this association is sensitive to cell metabolic state.

HEXOKINASE I is the primary isoform of hexokinase found in brain (21), and a number of insulin-sensitive tissues (2, 18, 20) and tumorigenic cells (14, 17). The majority of this hexokinase appears to be associated with mitochondria in many of these cell types. Although up to 85% of brain hexokinase can be associated with mitochondria after tissue fractionation, it has been suggested that only a small amount of hexokinase is associated with mitochondria in astrocytes (11). When associated with mitochondria, the affinity of the enzyme for one of its substrates (ATP) is elevated, and sensitivity to inhibition by its product glucose-6-phosphate (G-6-P)[1] is lowered (23). Thus, the interaction of hexokinase I with mitochondria is proposed to be kinetically advantageous. Furthermore, the association of hexokinase with mitochondria is proposed to be regulated in vivo. This hypothesis is based on the observation that the interaction of hexokinase with mitochondria is sensitive to the concentrations of several ions and metabolites. The principal modulator of hexokinase binding to mitochondria may be G-6-P, since this metabolite will release hexokinase from isolated mitochondria (17, 23). This effect of G-6-P is counteracted by physiological levels of inorganic phosphate. From this and other in vitro evidence, it is postulated that the association of hexokinase with mitochondria is modulated in concert with changes in the rate of glycolysis (23). According to this model, inhibition of glycolysis leads to an increase in the concentration of G-6-P and release of hexokinase from mitochondria, thereby decreasing the activity of hexokinase I. Conversely, stimulation of metabolism by increasing cell work would decrease G-6-P, increase inorganic phosphate, and promote binding leading to an enhancement in the efficacy of hexokinase I. Although the modulation of hexokinase binding to mitochondria has been detailed in vitro, the hypothesis that hexokinase distribution is regulated in vivo remains controversial (8). In the present study, we have evaluated the subcellular distribution of hexokinase in an astrocyte cell line, and monitored the modulation of this distribution during alteration of cell metabolism, using monoclonal antibodies raised against rat brain hexokinase I and indirect immunofluorescence-imaging techniques.

1. *Abbreviations used in this paper*: G-6-P, glucose-6-phosphate; MITO IMP, inner mitochondrial membrane epitope; 2DG, 2-deoxyglucose; 2DG-6-P, 2DG-6-phosphate.

Materials and Methods

Cell Culture

Astrocytes were obtained after the second passage from J. L. Leonard (University of Massachusetts Medical Center, Worcester, MA). The primary cultures were prepared from embryonic rat brain as previously described

(9). Cells were grown in 10-cm^2 culture dishes using DMEM supplemented with 10% FBS, 1000 U/ml penicillin G, 10 mg/ml streptomycin sulfate, and without phenol red. Cells were used between passages 3 and 8 for all experiments described. For immunocytochemical experiments, cells were grown on 22-mm round coverslips, plated at an initial density of 10^6 cells/plate and used after cells had become confluent (10–14 d after plating).

Immunocytochemistry

Cells were fixed with 4% filtered paraformaldehyde in PBS (20 mM; pH 7.8) for 15 min. Plates were washed in phosphate buffer, and the unreacted fixative was quenched with 0.1 mM glycine. Cells were then permeabilized with 0.25% Triton in 10 mM sodium citrate buffer (pH 7.8) for 20 min. Monoclonal antibodies to hexokinase were kindly provided by John E. Wilson and Allen D. Smith (Michigan State University, East Lansing, MI), and have been previously characterized (26). In single-label experiments, cells were incubated with the primary monoclonal antibody (0.05 mg/ml), washed, and then incubated with a fluorophore labeled anti-mouse IgG. In the absence of permeabilization, no significant labeling with antibodies was observed. In dual-label experiments, two different monoclonal antibodies were used for the independent localization of mitochondria and hexokinase. The monoclonal antibody used for identification of mitochondria was raised to an inner membrane epitope (3), and was purchased from Bioproducts for Science (Indianapolis, IN). To label each antibody with a specific fluorophore conjugated anti-mouse IgG, a blocking step was used after fluorophore labeling of the first monoclonal antibody. Nonfluorophore labeled anti-mouse IgG was used as the blocking agent. This step assured that all free sites for anti-mouse IgG interaction were covered before the second series of monoclonal and secondary labeled antibodies. Thus, a typical dual-label experiment consisted of incubation with an antihexokinase monoclonal antibody followed by Texas red conjugated anti-mouse IgG (rabbit affinity purified), then unlabeled anti-mouse IgG (goat affinity purified). After this blocking step, cells were incubated sequentially with the monoclonal antibody to the inner mitochondrial membrane epitope (MITO IMP) and a fluorescein conjugated anti-mouse IgG (sheep). Fluorescein labeling observed after deletion of the second monoclonal antibody, provided a measure of the efficacy of the blocking step. Experiments were deemed acceptable only when fluorescein labeling in the blocked controls was comparable to that seen in cells incubated with the fluorescein-conjugated anti-mouse IgG alone.

Fluorescence Microscopy and Image Analysis

Confocal Microscopy. Fluorophore-labeled antibodies were used to identify the subcellular location of mitochondria and hexokinase in fixed cells. To analyze the amount of hexokinase that was associated with mitochondria within a cell, information concerning the distribution of the respective fluorescent markers throughout the cell was required. This was necessary because the distribution of mitochondria is nonuniform with some areas of the cell being rich in mitochondria and others relatively mitochondria free. To analyze the three-dimensional (3D) distributions of hexokinase and mitochondria, a confocal microscope was used to acquire sequential through-focus images of labeled cells. A laser-scanning confocal microscope (model MRC-500; Bio-Rad Laboratories, Richmond, CA) equipped with a planapo oil (63X) immersion lens (n.a. = 1.4) was used for these experiments. The confocal microscope, unlike standard widefield microscopes, directly rejects out-of-focus light providing improved resolution along the z-axis at a cost to signal/noise (21). The aperture size of the confocal pinhole determines the relation between z-axis resolution and the signal/noise characteristics of the microscope (25). In the present work, pinholes on the microscope, for both fluorophores, were set to allow collection of ~80% of the emitted light observed when pinholes are opened completely. These settings provided a full width at half maximum integrated intensity (image plane depth of field) of ~0.9 μm (21). 3D image sets were obtained by acquiring 8–10 optical slices at 0.5-μm intervals. Dual-wavelength images were acquired using 488-nm excitation and two independent transmission filters, one centered at 525-nm (fluorescein) and the other a 600-nm long pass filter (Texas red). Before analysis, all images were corrected for dark current and instrument background. The contribution of fluorescence from the fluorescein signal to the image of Texas red was small, and did not significantly alter the estimated values for hexokinase distribution. Correction for the contribution of fluorescence from the fluorescein signal into the Texas red channel was evaluated according to the equation (expression 1) $F_{tr} = (I_{tr} - I_f * a)/(1 - a * b)$ where I refers to measured fluorescence intensity, F the noncontaminated signal (no spillover), and coefficients a and b refer to the % leakthrough of the fluorescein signal into the Texas red window, and the reciprocal spillover of Texas red signal into the fluorescein channel, respectively. Subscripts: f, fluorescein; tr, Texas red. Expression (I) is derived from the simultaneous solution of the equations which describe the origin of fluorescence signal in each channel: $I_{tr} = F_{tr} + F_f * a$, and $I_f = F_f + F_{tr} * b$. We determined that coefficients a and b were equal to 0.11 ± 0.2 (n = 6) and 0.09 ± 0.1 (n = 6) by measuring the fluorescence leakthrough from singly labeled samples. These values for percent spillover are specific for the gain and black level settings chosen for this experiment on our confocal microscope. From expression I, the Texas red signal can be corrected for spillover from fluorescein in any dual label image set using the measured values of fluorescence intensity in each channel (Ix) and the previously determined coefficients. Independent correction of the Texas red signal values for the entire cell image and the mitochondrial masked portion of the image allowed us to determine that spillover would lower the estimated values of % hexokinase bound to mitochondria by <5%. Results presented in the text are not corrected for spillover because this correction is small under the conditions of this experiment. All images were acquired within 6 h of sample preparation to assure sample stability.

Photobleaching of Sample. The rate of photobleaching during image acquisition was determined by measuring the rate of decrease in emitted light intensity from a uniformly fluorescent sample during the identical protocol used to collect the 3D data sets from labeled cells. To imitate the photobleaching of a labeled cell, a uniformly fluorescent sample was prepared. The sample was 3% gelatin labeled with the appropriate fluorophore by incubation for 30 min while cooling to 25°C with the succinimidyl ester derivative of the fluorophore. The measured rate of photobleaching is dependent on the characteristics of the specific imaging protocol. In experiments, a single image scan took 0.125 s, and 20 scans were averaged for a single plane of focus. Therefore, the bleach rate given is a measure of bleaching which occurs over integrals (frames) which is related to an absolute constant of 2.5 s/image frame. Using this procedure we found that, for Texas red, the rate of decline in fluorescence intensity as a function of the image frame fit an exponential function with a decay constant of −0.0055%/frame. The value for the rate of photobleaching was used to scale sequential image frames from cells where hexokinase was labeled with Texas red. The rate of photobleaching of fluorescein was very high thereby making the fluorescein signal difficult to quantitate. For this reason hexokinase was always labeled with Texas red. Correction for photobleaching was not carried out for the fluorescein anti-IMP images, since these images were used simply to provide a map of mitochondrial location and not for quantitative signal analysis.

Correction for Nonspecific Label. There was a uniform and low level of nonspecific fluorescence labeling in the cell because of the use of fluorophore-conjugated anti-mouse IgGs to label the primary monoclonal antibodies. To obtain an estimate of the actual amount of specific labeling, a value for the level of this nonspecific labeling must be subtracted from all hexokinase-specific images. In algebraic terms: the fraction of hexokinase which is associated with mitochondria in a given cell = $(\Sigma im - [NS * Pm]) / (\Sigma ic - [NC * Pc])$, where i represents the intensity value of individual pixels, i is the sum of pixel intensities, NS is the mean grey level of nonspecific fluorescence, and P is the number of picture elements associated with the mitochondria (subscript m) or the entire cell (subscript c). Nonspecific fluorescence associated with the hexokinase image was assessed by two methods: (a) in several experiments cells were incubated with the Texas red anti-mouse IgG alone, and therefore, no specific labeling was present in these samples. 3D image sets were obtained from multiple cells, then background subtracted and corrected for photobleaching. An average intensity value for nonspecific labeling was then calculated from these bleach corrected images; and (b) previous evidence suggested that the specific labeling of hexokinase in the nuclei of neural tissue (22) and astrocytes (11) was negligible. In our experiments, it also was determined that antihexokinase does not significantly label the nucleus. To test this cells were incubated with both secondary fluorophore labeled anti-mouse IgGs in the absence of a primary monoclonal antibody (both nonspecific labeling), or with specific labeling of the antihexokinase with Texas red. The level of labeling in distinct subcellular regions was compared between the fluorescein image (nonspecific label), and the Texas red image of the same cell (either specific or nonspecific label). When antihexokinase was present, the Texas red/fluorescein ratio in cytosolic regions was 100–10,000-fold higher than that measured in cells with the antihexokinase omitted. On the other hand, the ratio of Texas red/fluorescein fluorescence in nuclear regions was not significantly different when cells were specifically labeled with antihexokinase Texas red. Thus, specific labeling of the nucleus with antihexo-

kinase is insignificant. The absolute fluorescence intensity in the nucleus was 20% greater than in the cytoplasm (nonnuclear regions) in cells incubated with the Texas red-conjugated secondary antibody alone. This difference is likely because of a higher capacity of nuclear material to bind secondary antibody "nonspecifically". Nuclear values were scaled by this factor before use in correcting for nonspecific labeling. Based on these findings, intensity of fluorescence in the nucleus was used as a measure of nonspecific labeling in individual cells.

Determination of Mitochondrial Location and Associated Hexokinase. Mitochondrial-associated hexokinase was determined by first constructing a binary mask of mitochondria location from the image of fluorescein-labeled anti-MITO IMP, as described below. This mask was then used to evaluate the distribution of hexokinase in the bleach-corrected hexokinase image from the same cell. Since only mitochondria were specifically stained in the fluorescein image, an intensity threshold could in theory be used to remove the nonspecific labeling. However, there was some heterogeneity in the intensity of staining between individual mitochondria which made it difficult to set a global intensity threshold without introducing error in the assignment of pixels corresponding to mitochondria, particularly those that were lightly labeled. To compensate for the different levels of labeling of individual mitochondria, the intensity distribution of light from all regions within the image was first adjusted using a locally adaptive histogram equalization algorithm (16). A single global intensity threshold could then be chosen to eliminate most of the nonmitochondrial background without significant loss of mitochondrial regions. To remove the remaining nonmitochondrial pixels, data sets were searched in 3D for pixels which had no more than one neighbor, indicating that they were from random noise and not mitochondria. These isolated pixels were removed from the data set to provide a 3D spatial map of mitochondrial distribution within a cell. A binary mask was prepared by assigning a value of one to all pixels that remained in the data set, i.e., those associated with mitochondria. Subsequent multiplication of the hexokinase image with the binary mask provides a final image which represents only the hexokinase that is associated with mitochondria. This image of mitochondria-associated hexokinase was normalized to the total amount of hexokinase (nonmasked image) in the same cell to provide a measure of the fraction of hexokinase which was associated with mitochondria at the time of fixation.

Metabolite Measurements

G-6-P was measured in cell suspensions. Cells were removed from culture flasks with a plastic cell scraper and incubated at 37°C at a density of $\sim 10^7$ cells/ml. Suspensions were analyzed for cell density, protein mass, and cell volume. Cell density was measured in the presence of 0.25% trypsin using a hemocytometer, and cell volume was estimated from the volume of the cell pellet following centrifugation in hematocrit tubes (13). Cell mass was assumed to account for ~5% of total cell volume the remainder being water. Metabolic inhibitors were added directly to the suspensions. Experiments were terminated by the addition of TCA (final concentration 0.1%) and centrifugation at 8,000 *g* for 5 min. The supernatant was neutralized by the addition of a small amount (<1% vol/vol) of Tris buffer (pH 12), then analyzed for G-6-P content using an enzyme-linked spectrophotometric assay (10). Since 2-deoxyglucose (2DG) inhibits G-6-P utilization by G-6-P dehydrogenase contained in the assay system, the samples were allowed to incubate in the assay buffer for 20 min at room temperature before analysis. Time course studies showed that this period was sufficient to allow for complete enzymatic oxidation of the G-6-P without any significant decrease in absorbance of control samples.

Cell Fractionation

Procedures used for fractionation are essentially those reported by Blackshear et al. (4). Cells were scraped from culture flasks in medium containing (mmol/liter): sucrose, 350; EGTA, 0.5; Hepes, 10; pH 7.4 (condition A), or in the same Hepes-sucrose-based medium without EGTA, but containing $MgCl_2$, 1.5; and NaH_2PO_4, 1.0 (condition B). Cells in suspension were disrupted using a Dounce homogenizer with a Teflon pestle. The homogenate was centrifuged at 3,500 *g* for 5 min to collect nuclei and unbroken cells. The resulting supernatant was centrifuged at 20,000 *g* for 20 min to collect the mitochondrial and plasma membrane fragments. Finally, the remaining supernatant was centrifuged at 115,000 *g* for 60 min to separate the remaining microsomal particles from the soluble cell fraction (aqueous cytosol). Triton X-100 was added to the cytosolic fraction to a final level of 0.1%. All pellets were resuspended in fractionation media containing 0.1% triton. Hexokinase activity was measured in all fractions using the standard enzyme-linked assay (10). Data are expressed as a percent of the sum of hexokinase activity found in the three primary fractions; mitochondrial, microsomal, and cytosolic. These three fractions accounted for >90% of the activity in the original homogenate. The remaining activity was likely to be associated with unbroken cells residing in the slow speed pellet after homogenization.

Materials

Cell culture media, FBS, and penicillin/streptomycin sulfate solution were purchased from Gibco Laboratories (Grand Island, NY). Fluorophore-labeled antibodies were obtained from Calbiochem-Behring Corp. (San Diego, CA), and unlabeled anti-mouse IgG was purchased from Amersham Corp. (Arlington Heights, IL). All substrates, sugars, and metabolic inhibitors were purchased from Sigma Chemical Co., (St. Louis, MO). All other chemicals were of analytical grade and were obtained from commercial sources.

Mathematical Treatment of Data

Data are presented as means ±SEM. Statistical differences between means were determined using an unpaired *t* test. $P < 0.05$ was taken as a statistically significant difference between group means.

Results

Localization of Hexokinase by Immunofluorescence Cytochemistry

Two monoclonal antibodies were used to analyze the subcellular distribution of endogenous hexokinase in paraformaldehyde-fixed astrocytes. These antibodies designated 21 and 2B are directed against epitopes located in the NH_2-terminal half of the hexokinase molecule (26). Hexokinase is found to be highly localized within the astrocytes using either monoclonal antibody (Fig. 1; and see Fig. 3 *B*). The regions of dense staining resemble mitochondria seen in other cells. To determine if the localized hexokinase was specifically associated with mitochondria, we used several markers for analyzing the subcellular distribution of these organelles.

Mitochondrial Location

The dye rhodamine 123 was used to observe mitochondria and their distribution in living astrocytes. Rhodamine 123 partitions into mitochondria because of the high transmitochondrial membrane potential difference (5), and therefore, may be used to determine mitochondrial location in living cells. As seen in Fig. 2 *A*, mitochondria are heterogeneous in size, and distributed throughout the cell. Most mitochondria are found near the nucleus, with others less frequently found in the peripheral regions. To determine the spatial distribution of mitochondria in fixed cells, we used a monoclonal antibody raised against an inner mitochondrial membrane protein (anti-MITO IMP) (3). As shown in Fig. 2 *B*, the anti-MITO IMP displays a pattern of distribution within astrocytes which is similar to that observed with rhodamine 123 in living cells. Thus, the inner mitochondrial membrane antibody provides an excellent means to determine subcellular mitochondrial distribution.

Colocalization of Hexokinase and Mitochondria

To determine the extent to which hexokinase is associated with mitochondria in astrocytes, cells were incubated with antibodies to both mitochondria and hexokinase. These monoclonal antibodies were independently labeled with

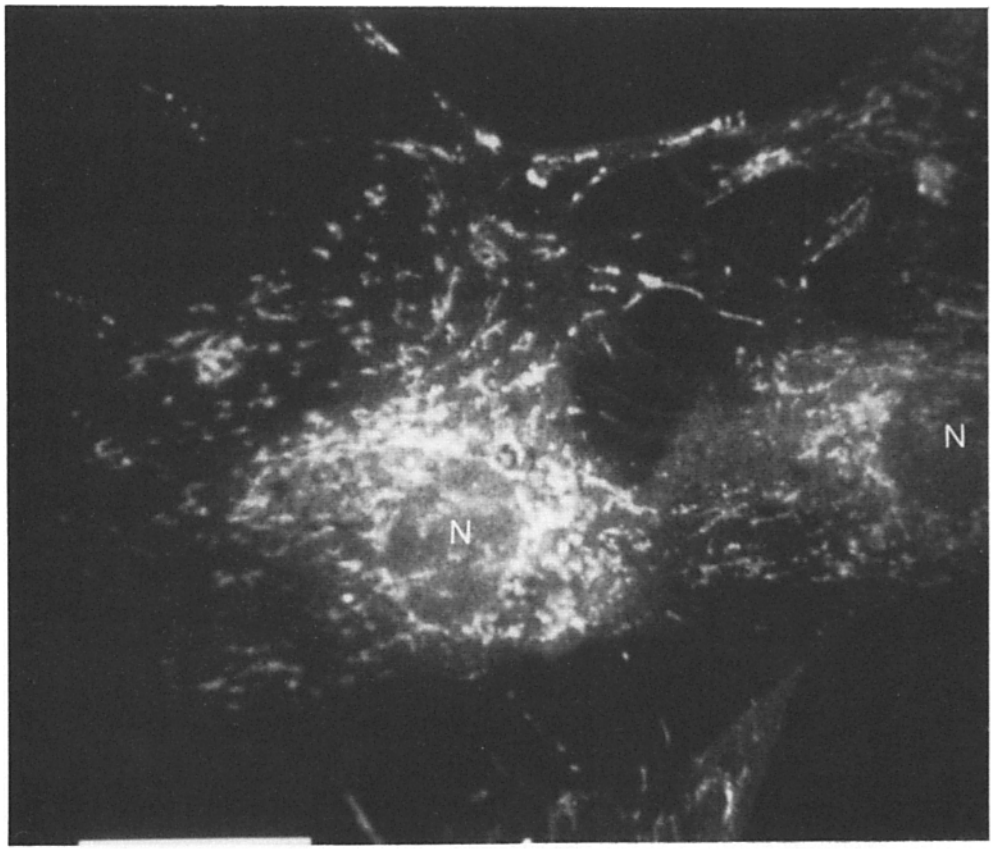

Figure 1. Confocal image of the distribution of hexokinase in fixed astrocytes. Monoclonal antibody 2B was used to label endogenous cellular hexokinase. This is an original image obtained in single wavelength mode (rhodamine) with a total integration time of 2 min. Notice that much of the label is localized to regions that resemble mitochondria in shape. (*N*) nuclei. Bar, 25 μm.

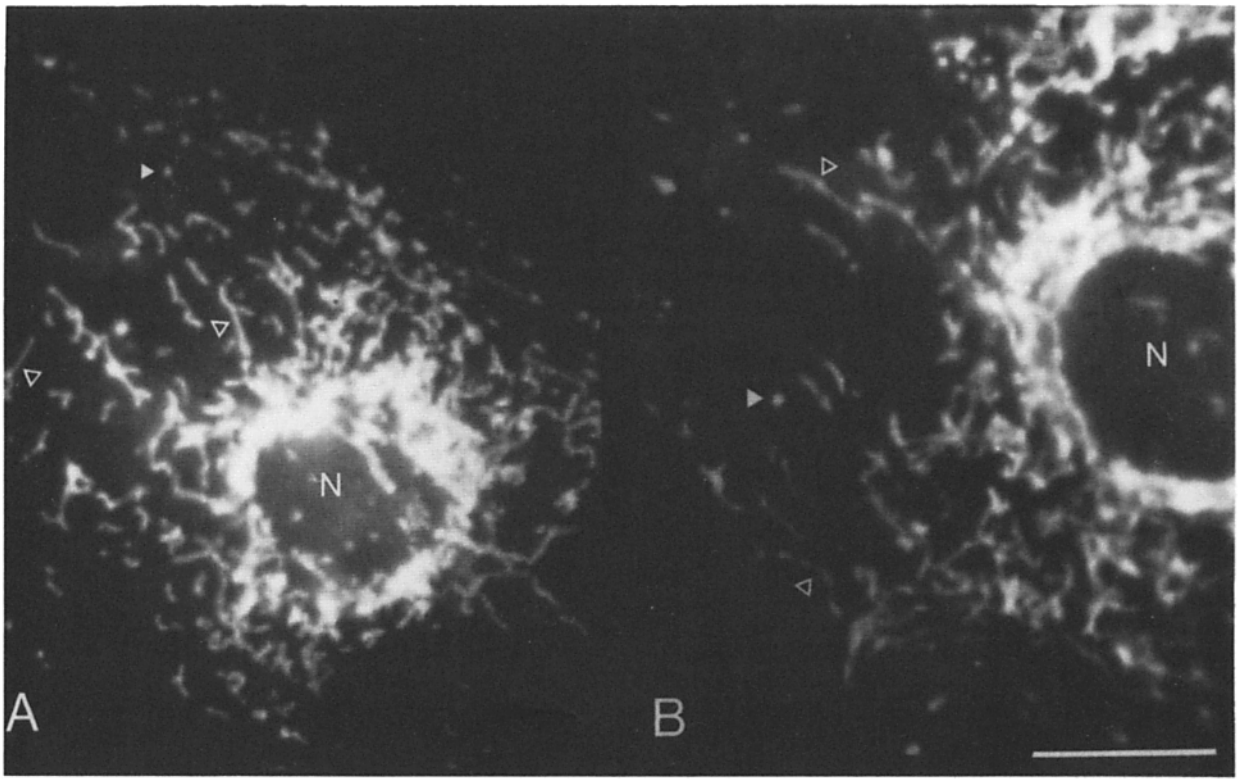

Figure 2. Fluorescence images of mitochondria in living (*A*) and fixed (*B*) astrocytes. (*A*) Rhodamine 123 labeled living astrocyte. Cell was incubated with 1 mg/ml rhodamine 123 for 1 min, then rinsed in physiological saline. Note that mitochondria have several characteristic shapes being either punctate in appearance (*dart*), or 2–3-μm long (*arrows*). (*B*) Anti-MITO IMP labeled fixed astrocyte. Note that the antimitochondrial marker recognizes structures identical in shape to those labeled with rhodamine 123. Images were acquired using a Photometrics CCD camera mounted on a microscope (model IM-35; Zeiss, Oberkochen, FRG). Bar, 10 μm.

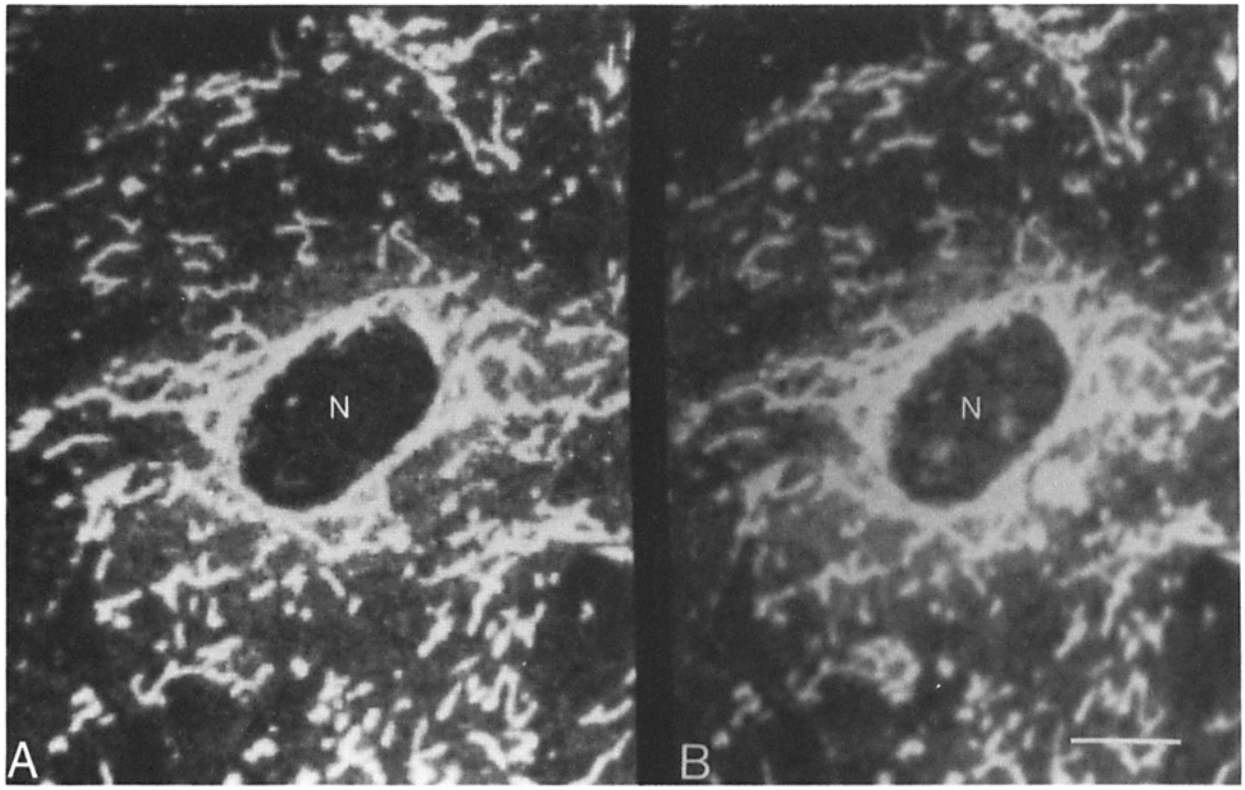

Figure 3. Confocal images of a fixed astrocyte labeled with antihexokinase, and anti-MITO IMP. The images shown result from the projection onto a single image plane of eight nonprocessed through focal images of the cell taken at 0.5 μm intervals. (*A*) Distribution of the anti-MITO IMP labeled with fluorescein. (*B*) Hexokinase distribution assessed using the monoclonal antibody 21 with a Texas red secondary label. Note the high degree of correspondence between the regions with a high density of hexokinase (*B*) and the mitochondria (*A*). Bar, 10 μm.

fluorescein or Texas red conjugated-secondary antibodies, respectively (see Materials and Methods). The distributions of the two fluorophore-labeled antibodies were analyzed simultaneously and independently using a confocal microscope. As seen in Fig. 3, points of high hexokinase localization align with regions determined to be mitochondria by the anti-MITO IMP. Although hexokinase appears to be primarily associated with mitochondria, a significant level of more uniformly distributed fluorescence is also observed. This low level of uniform fluorescence is in part related to nonspecific labeling by the fluorophore-conjugated anti-mouse IgG, as well as, some level of nonlocalized specifically labeled hexokinase. Fig. 4 *A* shows the distribution of hexokinase in the image plane where the majority of mitochondria reside. This image is corrected for nonspecific labeling using a mean intensity value obtained from the nucleus of this cell. Fig. 4 *B* shows the binary mitochondrial mask prepared from the image of the fluorescein-labeled anti-MITO IMP in this cell. Multiplication of these two image sets provides a final image set of the cellular hexokinase which is associated with mitochondria in three dimensions. The amount of hexokinase in this 3D data set is compared to the amount of hexokinase in the entire cell to obtain an estimate of the amount of cellular hexokinase which is associated with mitochondria at the time of fixation. In two independent experiments the amount of total cellular hexokinase associated with mitochondria was found to be 72.7% (Table I) and 64.6 $\pm$ 5.2% (SEM; n = 8) using the nuclear intensity of each cell as a correction for nonspecific labeling. Similar values for mitochondria-associated hexokinase were obtained when nonspecific labeling was estimated from multiple cells incubated only with the Texas red-conjugated anti-mouse IgG (Table I). Thus, both measures of nonspecific labeling provide similar estimates of percent hexokinase associated with mitochondria. However, use of the nuclear value on a cell by cell basis provides a significant decrease in variability, as indicated by the lower SD of the measurement (Table I). Without correction for nonspecific labeling, values for mitochondrial-associated hexokinase of 35.6% and 30.6 $\pm$ 1.7% are calculated for these two experiments. Therefore, at minimum 30–40% of the cellular hexokinase is localized to mitochondria. However, based on the good agreement between two independent measures of nonspecific fluorescence, it is likely that ~70% of the cells hexokinase is associated with mitochondria in these astrocytes under basal metabolic conditions.

Modulation of Hexokinase Distribution

The specific localization of hexokinase with mitochondria is proposed to be modulated in association with changes in the rate of glycolysis (23). G-6-P has been shown to modulate binding of hexokinase to mitochondria in vitro, suggesting a primary regulatory role. Under control conditions (10 m M glucose), G-6-P is ~0.2 m M (0.24 + 0.2 mM; n = 6), as measured in cells incubated in suspension. G-6-P concentration was altered by incubation with the inhibitor of glycol-

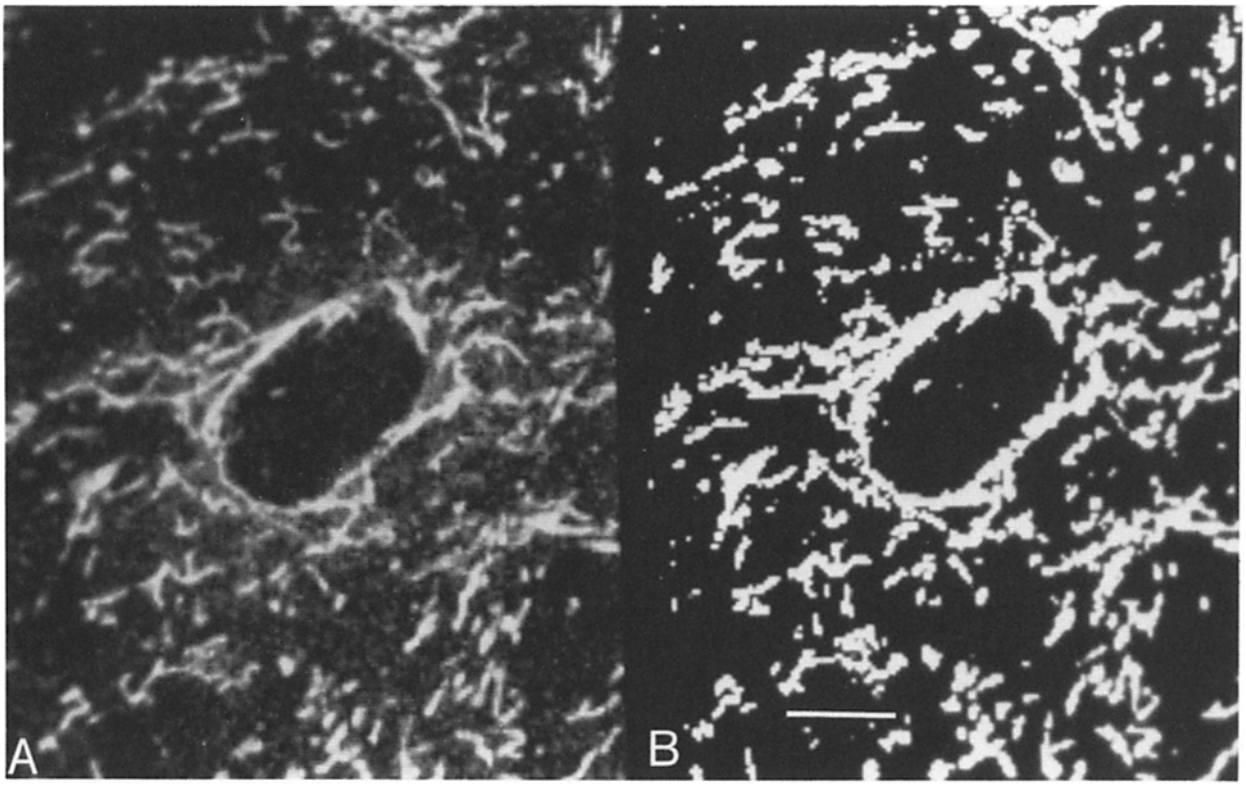

Figure 4. Confocal images of a fixed astrocyte labeled with antihexokinase, and anti-MITO IMP. The images shown are of a single focal plane from a through focal series. The plane shown corresponds to that having the highest density of mitochondria. (*A*) Distribution of antihexokinase. This image has been digitally corrected for nonspecific labeling using information regarding the intensity of nuclear fluorescence, as described in Materials and Methods. (*B*) Represents the binary mask for mitochondrial location prepared from the anti-MITO IMP distribution, as described in Materials and Methods. Bar, 10 μm.

ysis, 2DG (10 mM), in the presence of lowered glucose (1 mM). 2DG elicits a fourfold increase in G-6-P in suspended cells after 1 h (0.94 + 0.13 mM; n = 3). Images of hexokinase and mitochondrial location were acquired from control and 2DG-treated cells, and then analyzed for the percent of cell hexokinase associated with mitochondria. 1 h of incubation with 2DG resulted in an ~35% decrease in the amount of hexokinase associated with mitochondria (Table I). The distribution of hexokinase in the central image plane of a control and 2DG-treated cell is shown in Fig. 5. The total amount of hexokinase in the 3D data sets of these two cells is approximately equal, however, the amount of hexokinase associated with mitochondria was 81% in the control and 39% in the 2DG-treated cell. Fig. 6 shows images of the mitochondrial-associated, and nonmitochondrial-associated hexokinase in the central focal plane from these two cells in pseudocolor (a linear color scale has been used to show the level of hexokinase localized within the images). As can be seen, mitochondria are densely labeled with hexokinase in the control cell but less so in the 2DG-treated cell. On the other hand, there are no obvious regions of localization of hexokinase in the nonmitochondrial images. Since there is a 35% decrease in the amount of hexokinase associated with mitochondria after treatment with 2DG, it is likely that the released hexokinase is uniformly distributed throughout the cell and not sequestered into other distinct structures.

*Table I. The Percent Hexokinase Associated with Mitochondria**

	Control	2DG
Method of Correction for Nonspecific Label		
No correction	35.6 ±2.1	25.1 ±1.7
Estimate from non-specific labeled cells	62.3 ±5.2	45.5 ±4.2
Estimate from nuclear region of each cell	72.7 ±3.2	46.4 ±3.8
n	(10)	(9)

* Hexokinase associated with mitochondrial mask. Total cell hexokinase in 3D cell data set.
±SEM; (n) number of images analyzed.

Hexokinase Distribution Assessed from Fractionation Studies

Previous studies based on fractionation techniques indicated that a large proportion of hexokinase was associated with the soluble phase of primary astrocytes (80% cytosol), and only 20% with the total cell particulate fraction containing mitochondria (11). However, our immunocytological evidence demonstrates that for the most part hexokinase is associated with mitochondria in astrocytes. To determine if differences

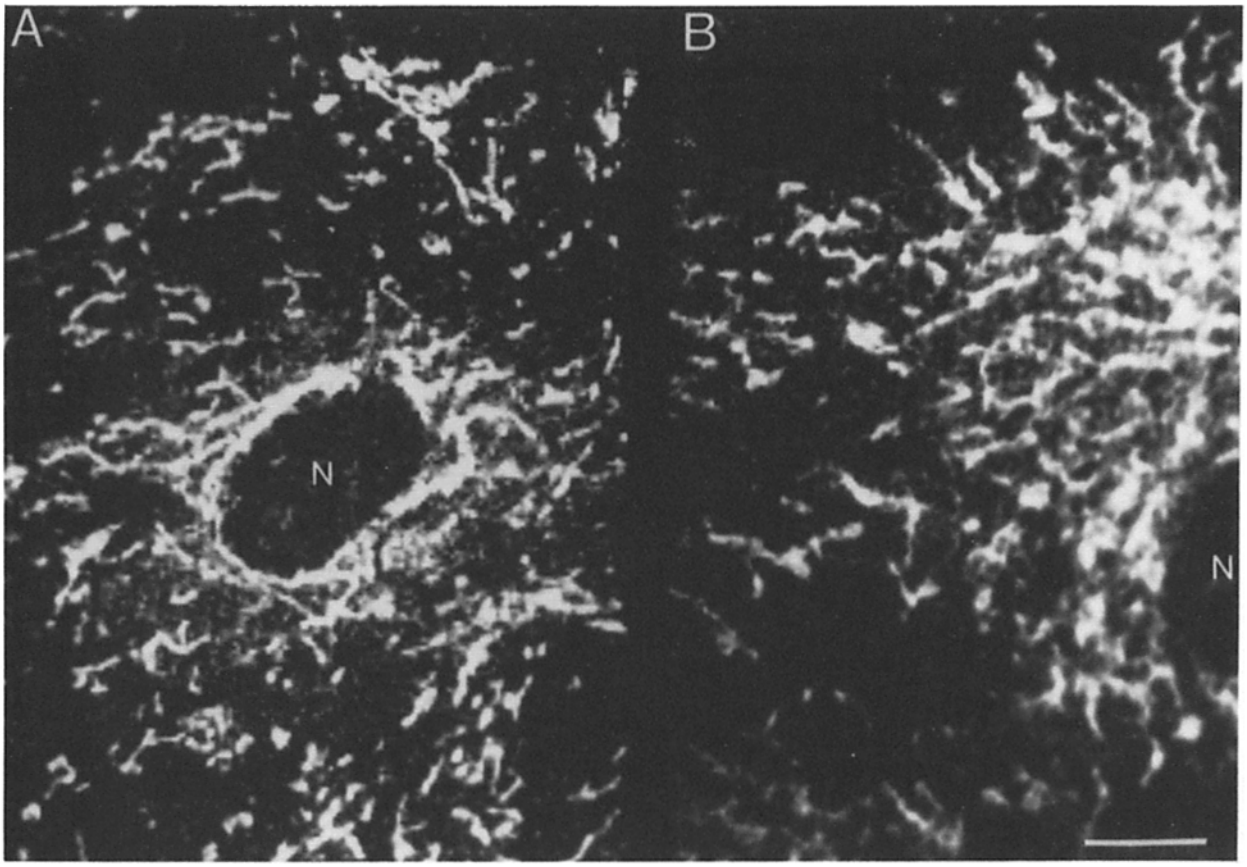

Figure 5. Confocal images of fixed astrocytes labeled with antihexokinase. Shown are single image planes of hexokinase distribution from a cell incubated with 10 mM glucose (*A*), and a cell treated with 2DG for 1 h before fixation (*B*). These are original images to which no processing has been applied. The percent hexokinase associated with the mitochondria was 81% for the control cell (*A*) and 39% for the 2DG-treated cell. The total intensity of fluorescence from the Texas red labeled antihexokinase in the 3D-image sets was similar for both cells.

in the observed distributions reflect differences in cell types used, or are associated with fractionation, primary astrocytes were fractionated under conditions similar to those used in the previous report and hexokinase activity was assessed in each fraction. As seen in Table II, ~80% of the cell hexokinase activity was found in the soluble phase. Only a minor amount (~15%) of hexokinase was found in the high speed particulate fraction which contained both mitochondria and plasma membrane particles. It is possible that the low level of hexokinase associated with the mitochondrial fraction is related to the specific conditions under which the cell fractionation was performed. For example, the fractionation experiment in Table II, condition A was carried out in media containing EGTA without Mg^{2+}. However, Mg^{2+} has been shown to promote hexokinase association with isolated mitochondria (17, 23). To test if fractionation conditions could affect the measured hexokinase activity in the mitochondria fraction, a second fractionation experiment was performed in the presence of promoters of hexokinase binding to isolated mitochondria. In the presence of Mg^{2+} and inorganic phosphate there was a significantly higher percentage of hexokinase in the mitochondrial fraction (36%). In addition, there was an increase in the amount of hexokinase found in the microsomal pellet (Table II; condition B). This later finding may be due to the collection of submitochondrial membranes containing hexokinase in the microsomal pellet, or a specific association of hexokinase with another membrane component in this fraction. If the activity in the microsomal fraction is assumed to be of mitochondrial origin, then at most 45% of the cells' hexokinase is found to be associated with mitochondria when fractionation is carried out in the presence of Mg^{2+}. Under either fractionation condition, values for mitochondrial-associated hexokinase were significantly lower than estimates made using the imaging approach with these primary astrocytes.

Discussion

In the present work, we have demonstrated that hexokinase isozyme I is associated with mitochondria in glial cells maintained in culture. Our estimate based on immunocytochemical studies is that ~70% of the cells' complement of hexokinase I is associated with mitochondria under basal metabolic conditions. This estimate is considerably higher than that based on fractionation studies carried out with these cells in the presence or absence of factors which promote hexokinase binding in vitro (Table II; also see reference 11). While fractionation studies provide valuable analysis of the distributions of tightly bound or integral membrane proteins, it appears that such methods may be less reliable for molecules whose associations with subcellular surface appear to be regulated. Since fractionation studies require disruption of

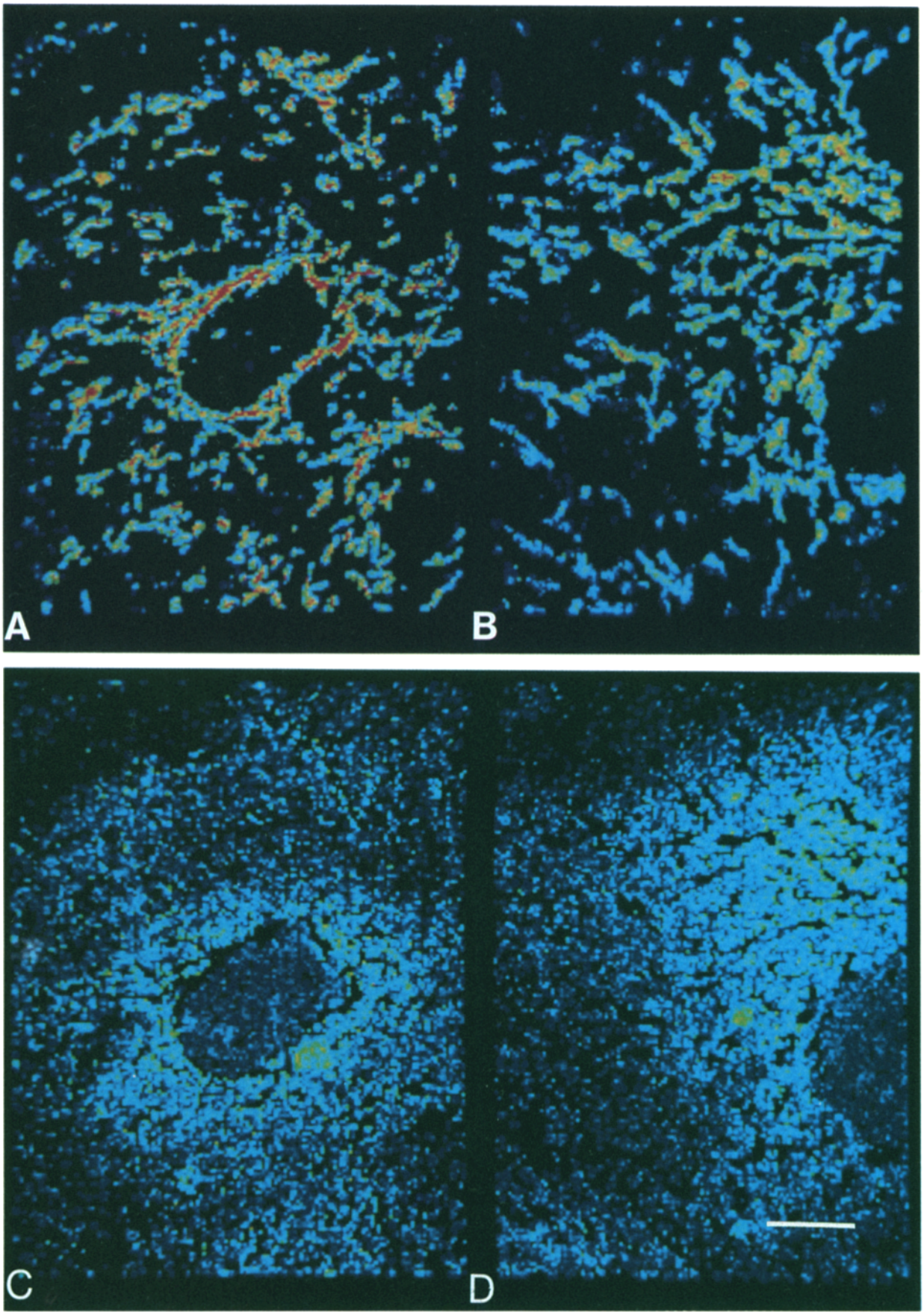
A
B
C
D

Table II. Hexokinase Activity in Cell Fractions

	Mitochondria plasma membrane fraction	Microsomes	Cytosol
	% Total Hexokinase Activity		
Condition A	15.9%	3.1%	81.0%
± SEM	1.8	0.6	7.1
Condition B	34.6%	7.8%	55.8%
± SEM	1.0	0.5	4.0

Condition A. Hepes-sucrose buffer with EGTA. Condition B: Hepes-sucrose buffer; no EGTA with Mg^{2+} and inorganic phosphate. Fractions were prepared as described in methods. SEM are based on at least triplicate measurements performed on all fractions prepared in a single experiment.

the cell and replacement of the "cytosol" with a physiological buffer, it is likely that hexokinase distribution is altered during the fractionation procedure depending on the exact nature of the fractionation media (Table II). Thus, a primary advantage of the imaging approach is that hexokinase is presumably fixed into place within the cell before analysis. In this respect, the ability to quantitate the relative distribution of a protein at a specific site in a fixed preparation may be of general use for assigning location to enzymes whose distributions may be dynamic.

It could be argued that the high relative levels of hexokinase associated with mitochondria is caused by preferential loss of the unbound enzyme during preparation of samples before imaging. Several findings indicate that the unbound component of hexokinase is not lost during sample preparation. First, free hexokinase is found to increase after treatment with 2DG, indicating that free hexokinase is preserved. Second, hexokinase is not labeled significantly with antihexokinase if cells are not permeabilized, yet immunoblots of fixed and fixed and permeabilized samples indicate that no significant loss of hexokinase occurred during the permeabilization procedure (data not shown). Thirdly, fluorescently labeled native hexokinase localizes to mitochondria following its injection into living astrocytes, and fixation does not elicit a visible change in this distribution (unpublished observations). Thus, the antibody labeling procedure appears to provide an adequate measure of the distribution of endogenous hexokinase at the time of fixation.

The release of hexokinase from mitochondria observed after treatment with 2DG indicates that hexokinase localization can be modulated in the intact cell (Table I; Fig. 6). In vitro studies of hexokinase association with isolated mitochondria suggest that hexokinase binding to mitochondria is sensitive to many factors including the concentrations of certain metabolites (G-6-P; Pi) and ions (Mg^{2+}; H^+). For example, hexokinase bound to mitochondria is released in the presence of millimolar amounts of G-6-P. On the other hand, physiological levels of Mg^{2+} or Pi promote binding and reverse the G-6-P effect (17, 23). Fractionation data presented in Table II are consistent with these previous observations. These observations have led to the hypothesis that changes in the rate of glycolysis modulate hexokinase binding to mitochondria. Since the levels of and interactions between the various effectors in vivo are not known with certainty, questions remain concerning the modulation of hexokinase distribution in response to changes in cell metabolism (8). 2DG was used to inhibit glycolysis in astrocytes before fixation. 2DG is phosphorylated to 2DG-6-phosphate (2DG-6-P) by hexokinase, but is not metabolized further. As 2DG levels increase within the cell, the rate of G-6-P removal by hexose isomerase and G-6-P dehydrogenase decrease because of inhibition by 2DG-6-P. After 1 h of incubation with 2DG, G-6-P levels increased fourfold, and therefore, 2DG-6-P levels also are presumed elevated. Thus, the significant decrease in mitochondrial-associated hexokinase that occurred in the presence of elevated G-6-P (Table I; Fig. 4) is consistent with the hypothesis that hexokinase distribution can be modulated in association with changes in cell metabolism.

Alterations in the kinetic properties of hexokinase caused by its association with the outer mitochondrial membrane have been reported. The bound form of hexokinase exhibits a higher affinity (lower K_m) for ATP (24), and a decreased susceptibility to inhibition by G-6-P (19) than does the soluble form. In addition, for hexokinase bound to mitochondria isolated from ascites cells, the rate of hexokinase turnover (G-6-P production) is elevated when ATP is supplied from endogenous mitochondrial oxidative phosphorylation relative to ATP added to the incubation medium (1). These observations suggest that important kinetic and functional advantages are conferred through association of the enzyme with specific sites at the outer mitochondrial membrane. In light of these findings, it has been proposed that binding of hexokinase to the outer mitochondrial membrane leads to an increase in the efficacy of the hexokinase reaction (23). It should be noted that recent evidence suggests that hexokinase may not be directly bound to the outer mitochondrial membrane in brain, but rather on some other structure which cosediments with mitochondria during standard fractionation procedures (15). Based on our findings, this binding structure is either intimately associated with mitochondria in astrocytes, or these recent observations are specific for brain cells other than astrocytes.

Figure 6. Pseudocolor images of antihexokinase distribution in cells grown in normal medium and in the presence of 2DG. Images of mitochondrial associated (*A* and *B*) and nonmitochondrial associated hexokinase (*C* and *D*) from a control cell (*A* and *C*) and a cell treated with 10 mM 2DG for 1 h before fixation (*B* and *D*). The mitochondria-associated hexokinase images are prepared by multiplication of the respective binary masks with the antihexokinase images (Fig. 4). Nonmitochondria-associated hexokinase images are prepared by subtraction of the mitochondria-associated hexokinase image from the antihexokinase image (Fig. 5). A linear color scale is used with red indicating the highest levels of hexokinase and blue the lowest levels. Note the high density of labeling in the mitochondrial-associated hexokinase images relative to the nonmitochondria-associated hexokinase images. In images of nonmitochondrial hexokinase distribution there are few points of high hexokinase that can be observed. These points are likely to be mitochondrial regions which were not included in the mask by the algorithm used to generate it. This occurs occasionally due to weak staining of edges of mitochondria by the anti-MITO IMP. However, it is clear from the low number of these points that the mask provides an excellent indicator of mitochondrial location in the hexokinase images. Notice that nonmitochondrial hexokinase is low and uniformly distributed in both cells. Bar, 10 μm.

Historically, quantitation of protein localization at specific subcellular sites has been carried out by techniques, such as differential centrifugation, which require disruption of cell integrity. In the present report, we present an approach which uses indirect immunofluorescence and 3D-imaging techniques to simultaneously identify the distributions of specific structures and proteins under conditions were cell ultrastructure is maintained. The quantitation of relative distributions using this approach may be of general use, particularly in respect to proteins whose subcellular distributions may be dynamic.

Quantitative Confocal Microscopy

The approach that we have taken to assess the amount of hexokinase which is associated with discrete structures (mitochondria) relative to that which is uniformly distributed is based on our ability to acquire a series of high-resolution fluorescence images taken at regular intervals throughout a cell. This has been achieved in the present study with the use of a laser-scanning confocal microscope whose pinholes have been closed to the point where both good z-axis resolution and signal/noise are retained in each image of the 3D image series. Potentially, 3D data with similar or even better z resolution can be obtained using conventional wide-field microscopy coupled with appropriate image restoration to remove out-of-focus blurring (6). Use of such a system may be more appropriate for investigations of living systems where the low transmission characteristics and cell photodamage caused by continuous laser illumination may limit the use of the confocal microscope. However, a primary benefit of the confocal microscope is that it provides 3D information directly, thereby eliminating the need for additional postprocessing in these studies.

The ability to acquire images with limited contribution from out-of-focus light allows for evaluation of fluorophore distributions from through-focus image series with only minor correction. First, correction for photobleaching between sequential image planes was performed. Second, correction for nonspecific labeling of the cells by the fluorophore conjugated secondary antibodies was carried out. Two methods were used for estimation of the level of nonspecific labeling. Use of values obtained by either approach gave similar mean values for the percent of hexokinase associated with mitochondria. However, the usage of the mean grey level from a nuclear region as a correction factor significantly decreased the SE, indicating the usefulness of using a measure which can be applied on a cell by cell basis. Based on the present results, it is likely that 3D microscopy coupled with appropriate image processing as described in this paper will allow for analysis of the dynamic association of specific molecules with distinct subcellular structures in a wide range of biological questions.

In summary, we have used quantitative confocal microscopy and immunocytochemical techniques to investigate the subcellular distribution of hexokinase in astrocytes grown in culture. Approximately 70% of the hexokinase is associated with mitochondria in these cells under control conditions (10 mM glucose). After inhibition of glycolysis with 2DG the amount of hexokinase associated with mitochondria decreased by ~35%. Therefore, these findings support the hypothesis that a significant amount of hexokinase is colocalized with mitochondria in astrocytes in vivo, and that this specific distribution is dynamically modulated in response to changes in cell metabolic state.

We would like to thank John E. Wilson and Allen Smith (Michigan State University, East Lansing, MI) for their critical review of this work, as well as for kindly providing the hexokinase antibodies. We would also like to acknowledge the intellectual contributions of Drs. Walter Carrington and Larry Lifshitz (University of Massachusetts Medical Center, Worcester, MA) to this manuscript.

Generation and characterization of monoclonal antibodies to hexokinase were supported by National Institutes of Health NS 09910 (to J. E. Wilson). R. M. Lynch was the recipient of a Charles A. King Fellowship during the tenure of this study. This work was supported by grants from the National Institutes of Health (DK-32520) to the Diabetes and Endocrinology Research Center at the University of Massachusetts Medical Center, and HL14323 to F. S. Fay.

Received for publication 12 April 1990 and in revised form 23 October 1990.

References

1. Arora, K. K., and P. L. Pedersen. 1988. Metabolic significance of mitochondrial associated hexokinase in tumor cell metabolism: evidence for preferential phosphorylation of glucose by intramitochondrially generated ATP. *J. Biol. Chem.* 263:17422–17428.
2. Aubert-Foucher, E., B. Font, and D. C. Gautheron. 1984. Rabbit heart mitochondrial hexokinase: solubilization and general properties. *Arch. Biochem. Biophys.* 232:391–399.
3. Billet, E. E., B. Gunn, and R. J. Mayer. 1984. Characterization of two monoclonal antibodies obtained after immunization with human liver mitochondrial membrane preparations. *Biochem. J.* 221:765–776.
4. Blackshear, P. L., R. A. Nemenoff, and J. Avruch. 1983. Insulin and growth factor stimulate the phosphorylation of a Mr-22,000 protein in 3T3-L1 adipocytes. *Biochem. J.* 214:11–19.
5. Chen, L. B. 1988. Mitochondrial membrane potential in living cells. *Annu. Rev. Cell Biol.* 4:155–181.
6. Fay, F. S., W. Carrington, and K. E. Fogarty. 1989. Three-dimensional molecular distribution in single cells analyzed using the digital imaging microscope. *J. Microsc. (Oxf.).* 153:133–149.
7. Kao-Jen, J., and J. E. Wilson. 1980. Localization of hexokinase in neural tissue: electron microscopic studies of rat cerebellar cortex. *J. Neurochem.* 35:667–678.
8. Kyriazi, H. T., and R. E. Basford. 1986. An examination of the in vivo distribution of brain hexokinase between the cytosol and outer mitochondrial membrane. *Arch. Biochem. Biophys.* 248:253–271.
9. Leonard, J. L. 1988. Dibutyryl cAMP induction of type II 5'deiodinase activity in rat brain astrocytes in culture. *Biochem. Biophys. Res. Commun.* 151:1164–1176.
10. Lowry, O. H., and J. V. Passonneau. 1976. *In* A flexible system of enzymatic analysis. Academic Press Inc., Orlando, FL. pp. 174 and 194.
11. Lusk, J. A., C. M. Manthorpe, J. Kao-Jen, and J. E. Wilson. 1980. Predominance of the cytoplasmic form of brain hexokinase in cultured astrocytes. *J. Neurochem.* 34:1412–1420.
12. Deleted in proof.
13. Lynch, R. M., and R. S. Balaban. 1987. Coupling of aerobic glycolysis and Na-K ATPase in the renal cell line MDCK. *Am. J. Physiol.* 253*(Cell Physiol. 22)*:C269–276.
14. Parry, D. M., and P. L. Pedersen. 1983. Intracellular localization and properties of particulate hexokinase in Novikoff ascites tumor. *J. Biol. Chem.* 258:10904–10912.
15. Parry, D. M., and P. L. Pedersen. 1990. Glucose catabolism in brain. Intracellular localization of hexokinase. *J. Biol. Chem.* 265:1059–1066.
16. Pizer, S., J. D. Austin, R. Cromartie, G. Geselowitz, and B. H. ter Haar Romey. 1986. Algorithms for adaptive histogram equalization, S.P.I.E. (*Soc. Photop. Instr. Eng.*) 671:132–138.
17. Rose, I. A., and J. V. B. Warms. 1967. Mitochondrial hexokinase: release, binding and location. *J. Biol. Chem.* 242:1635–1645.
18. Sener, A., F. Mallaisse-Lagae, M. Giroix, and W. J. Mallaisse. 1986. Hexokinase metabolism in pancreatic islets: compartmentation of hexokinase in islet cells. *Arch. Biochem. Biophys.* 251:61–67.
19. Tuttle, J. P., and J. E. Wilson. 1970. Rat brain hexokinase: a kinetic comparison of soluble and particulate forms. *Biochim. Biophys. Acta.* 212: 185–188.
20. Walters, E., and P. McLean. 1968. Effect of anti-insulin serum and alloxan-diabetes on the distribution of multiple forms of hexokinase in lactating rat mammary gland. *Biochem. J.* 109:737–741.
21. Wells, K. S., D. R. Sandison, J. Stricker, and W. W. Webb. 1989. Quantitative fluorescence imaging with laser scanning confocal microscopy. *In* The handbook of biological confocal microscopy. J. Pawley, editor. Ple-

num Press, NY. 27–39.
22. Wilkin, G. P., and J. E. Wilson. 1977. Localization of hexokinase in neural tissue: light microscopic studies with immunofluorescence and histochemical procedures. *J. Neurochem.* 29:1039–1051.
23. Wilson, J. E. 1980. Brain hexokinase; the prototype ambiquitous enzyme. *Curr. Top. Cell. Regul.* 16:1–44.
24. Wilson, J. E. 1988. Function of ambiquitous proteins in a heterogeneous medium. *In* Microcompartmentation. D. P. Jones, editor. CRC Press Inc., Boca Raton, FL. 171–190.
25. Wilson, T. 1989. The role of the pinhole in confocal imaging systems. *In* The handbook of biological confocal microscopy, J. Pawley, editor. Plenum Press, NY. 113–126.
26. Wilson, J. E., and A. D. Smith. 1985. Monoclonal antibodies to rat brain hexokinase. *J. Biol. Chem.* 260:12838–12845.